Theoretical Validation of Reversible Acidochromism of a Cinnamaldehyde based Scaffold with Experimental Investigations

Rupam Patgiri[1], Bapan Saha[2], Nilpawan Sarma[3], Ziaur Rahman[4] and Ruhul Amin Bepari[1,*]

[1]Department of Chemistry, Bhattadev University, Bajali, Pathsala-781325, India
[2]Department of Chemistry, Handique Girls' College, Guwahati-781001, India
[3]Department of Chemistry, Gauhati University, Guwahati-781014, India
[4]Department of Chemistry, University of North Bengal, Raja Rammohunpur, Darjeeling-734013, India

*Corresponding author: E-mail: ruhulbepari@gmail.com

Present study explores the reversible acidochromism displayed by cinnamaldehyde derivative-based scaffold (**P1**), which is highly sensitive to variations in acidity and basicity. Upon exposing to an acidic environment, the solution containing **P1** undergoes a vivid colour shift from yellow to a vibrant pink-fuchsia colour due to the conversion of imine within **P1** into its quinonoid form. The color change can be completely reversed by adding a basic material, demonstrating the reversible acidochromic behavior of the **P1** system. Moreover, the practical application of this acidochromic property is demonstrated through the development of a test kit utilizing paper strips. This kit effectively harnesses the acidochromic nature of **P1** to detect even minute quantities of acidic or basic substances in solutions. The underlying mechanisms of the acid-base detection and corresponding colorimetric shifts in response to the acid-base interactions have meticulously been explored using density functional theoretical investigations.

Keywords: Acidochromism, Colorimetry paper, Strips.

INTRODUCTION

The acid-base equilibrium is known to significantly control numerous chemical and biochemical reactions occurring either in aqueous/non-aqueous or gas phase. Therefore, the determination of different types of acid–base equillibria has received paramount of interests in a diversified fields such as medical [1], food [2-4] or environmental analysis [5,6]. Both the elctro-analytical sensors (EAS) and optical chemical sensor (OCS) systems have widely been employed for the determination of the acid-base equillibria in many instances [7-15]. On the other hand, OCS have mostly replaced pH sensors due to their superior sensitivity, the ease of simple analysis, and online/remote sensing capabilities. The OCS are known to be non-toxic in nature, easy to handle and can be applied in hazardous environment as well as clinical diagnosis [16-18].

Depending upon the nature of signals emitted by the sensing materials the chemosensors can be classified into three categories *viz.* colorimetric sensors, fluorogenic sensors and electroche-

mical sensors. The Schiff base-based chemosensors fall into the colorimetric category and the signals arise from the changes that take place in their electronic structures due to various types of charge transfer processes such as ligand-to-metal charge transfer and metal-to-ligand charge transfer. The signals of these optical sensors are sensitive to the interactions between the metal ions and Schiff bases [19].

In context of non-aqueous solutions, the absorption-based optical sensors were developed to match the absorption characteristics of certain pH indicators [20]. Additionally, some organic dyes were reported to function as colorimetric indicators in non-aqueous media, enabling the determination of concentrations of colourless acids or bases [21]. However, studies focusing on the colorimetric visualization of acid-base equillibria and determination of acid dissociation constants in non-aqueous media are still scarce. The acid dissociation constant is a crucial parameter in routine chemistry research and its knowledge in non-aqueous media is essential for understanding the organic reactions [22-30]. In aqueous solvents, the high dielectric cons-

tant facilitates the rapid dissociation of acids due to reduced electrostatic interactions between the proton and the conjugate base [24,25]. In contrast, the dissociation of acids in non-aqueous solvents is less favourable in this regard, making it an area of interest for researchers in the contemporary research. While there are some reports available on the determination of acid dissociation constants in non-aqueous systems [22-24, 31-33], the use of suitable probe based spectroscopic methods remains limited. Most measurements have been conducted using conductometric or potentiometric methods with glass electrodes which involve various assumptions and disadvantages including frequent calibration, susceptibility to interference and corrosion issues [24,25,34]. To overcome these drawbacks, researchers have turned their attention towards the development of colorimetric acid-base sensors. The overlapping indicator method, using newly designed and synthesized indicators, shows promise in determining the prototropic dissociation constants of acids/bases in the non-aqueous solvents [24,35,36]. These colorimetric acid-base sensors offer high signal-to-noise ratios and physical stability, making them suitable for the quantitative analysis and practical applications.

Recently, Wakabayashi *et al.* [37] developed a novel synthetic route of 1- and 2-pyridylazulenes as well as 1,3-dipyridilazulenes with alternating positions of nitrogen atom present in the pyridine ring. They widely investigated the changes in colour upon the addition of acid or specific metal ions. Additionally, they demonstrated that a device containing multiple pyridylazulenes could function as an effective pH indicator. In present work, an effort has been made to design a cinnamaldehyde derivative **P1** and characterize it theoretically. The structures and spectra of cinnamaldehyde derivative **P1** were explored with using mordern theoretical tools *viz.* density functional theory (DFT) and its time-dependent counterpart (TD-DFT) in order to understand how an acidic environment affects its colour changing capabilities as well as its experimental study and practical applications. Further, the theoretical aspect is investigated experimentally by preparing the salen-type (**P1**) through a Schiff-base formation reaction involving 4-nitro-aniline and *N,N*-dimethyl cinnamaldehyde. To validate the practical applicability of **P1** as an acid indicator, a real-time paper strip test kit is developed for detecting minute quantities of acids in non-aqueous solvents.

EXPERIMENTAL

All the solvents and chemicals used in this work were of analytical reagent (AR) grade and procured from different commercial sources. Both *p*-nitroaniline and *N,N*-dimethyl cinnamaldehyde were purchased from the Sigma-Aldrich, USA. Prior to use, the solvents were dried further. All glasswares were thoroughly cleaned by concentrated sulfochromic acid followed by the repeated washing with double-distilled water. The UV-visible absorption spectra were recorded on a Hitachi U-2910 spectrometer. The ^{1}H NMR spectra were recorded on a Bruker 400 MHz spectrometer using DMSO-d_6 as solvent and tetramethylsilane (TMS) as an internal standard.

Solution preparation: Stock solutions of cinnamaldehyde derivative (**P1**) and trifluoroacetic acid (TFA) of concentrations

5×10^{-3} M and 5×10^{-4} M, respectively was prepared by dissolving suitable amounts of their compounds in acetonitrile (ACN).

Computational details: The Gaussian-16 programme package [38] was employed for the density functional calculations to investigate the validation of protonated sites. For the purpose, geometries were optimized at B3LYP-GD3/6-31++G (d,p) level of theory. The B3LYP is a Lee-Yang-Par (B3LYP) exchange-correlation functional, which has effectively been used in the study of geometrical parameters and molecular properties [30,39]. While, GD3 was used to encounter the dispersion interaction (if any) and 6-31++G(d,p) basis set is used as it incorporates sufficient polarized and diffuse function to produce reasonably accurate results [40,41]. To validate the presence of real minima, frequency calculation was performed on all the chosen geometries. For optical properties, UV-visible spectra of the systems were computed as vertical excitations from ground state geometries ($N = 20$ states) using time dependent density functional theory (TD-DFT). For solvent phase study, the polarizable continuum model (PCM) was used in acetonitrile ($e = 37.5$) [42]. It implements the self-consistent reaction field (SCRF) approach which reveals solvent polarization in terms of electrostatic potential. All these calculations were performed at the same level of theory. Furthermore, ^{1}H NMR spectra are computed at B3LYP/6-311+G(2d,p) level of theory with TMS as reference [43,44]. For purpose, Gauge Independent Atomic Orbital (GIAO) method is adopted.

RESULTS AND DISCUSSION

To validate the theoretical acidochromic behaviour of **P1**, few experimental investigations were also conducted to show the acidochromic behaviour of probe in a non-polar solvent like acetonitrile. Thus, the chemosensor *N,N*-dimethyl-4-(1*E*, 3*E*)-3-(4-nitrophenyl)imino)prop-1-en-1-yl)aniline (**P1**) was synthesized *via* the Schiff-base formation reaction of 4-nitro-aniline and *N,N*-dimethyl cinnamaldehyde in methanol using catalytic amount of acid (**Scheme-I**).

Colorimetric and UV-vis spectral analyses: Absorption spectra of the receptor **P1** were recorded in different solvents of low polarity. Fig. 1 illustrates the variation in absorbance of **P1** in acetonitrile when different acids were present. Although, the receptor molecule initially exists in imine form, it slowly converts into quinonoids form upon the addition of organic acids such as trifluoroacetic acid (TFA) or acetic acid (AcOH), as shown in the **Scheme-II**.

Since the imine and quinonoid forms have distinct absorption characteristics, so the actual colour of receptor depends on the relative proportion of two forms present in the system. The receptor solution normally appears as yellow but upon the addition of TFA it gradually turns into light pink indicating the conversion of imine to the quinonoid form (Fig. 1). However, a similar visual colour change is not observed with the use of AcOH at a concentration similar to TFA. It can clearly be seen from Fig. 1 that the absorption of imine form appearing at a shorter wavelength of $\lambda_{max} \approx 372$ nm steadily decreases but the absorption of the quinonoids form appearing at a longer wavelength of $\lambda_{max} \approx 558$ nm increases upon the addition of acids. This observation aligns with the theoretically investiga-
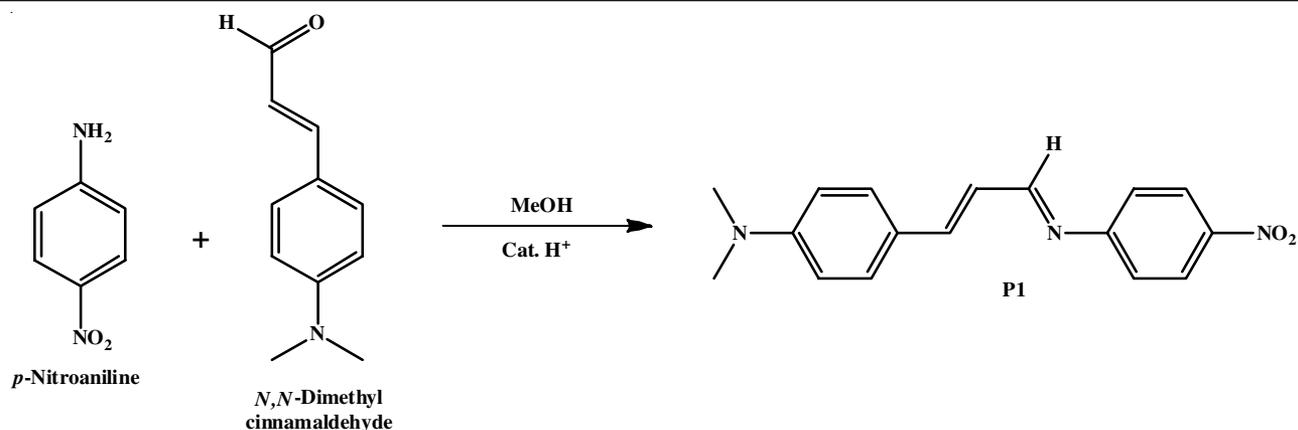
Scheme-I: Synthesis of *N,N*-dimethyl-4-(1*E*,3*E*)-3-(4-nitrophenyl)imino)prop-1-en-1-yl)aniline (**P1**)
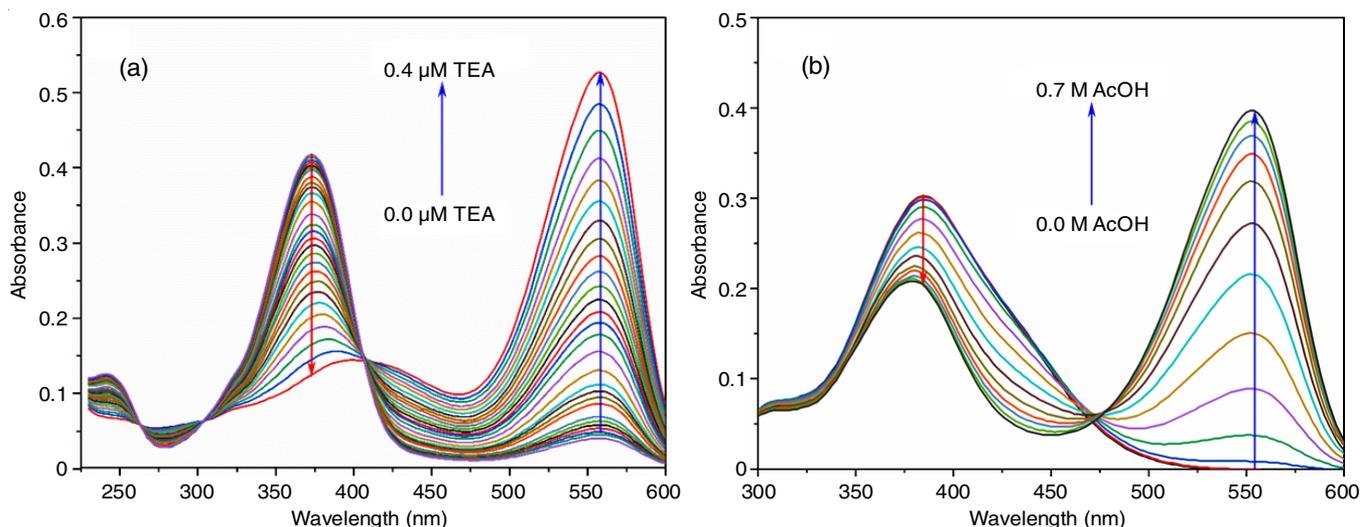
Fig. 1. UV-vis absorption spectra of **P1** in the presence of (a) TFA and (b) AcOH in ACN
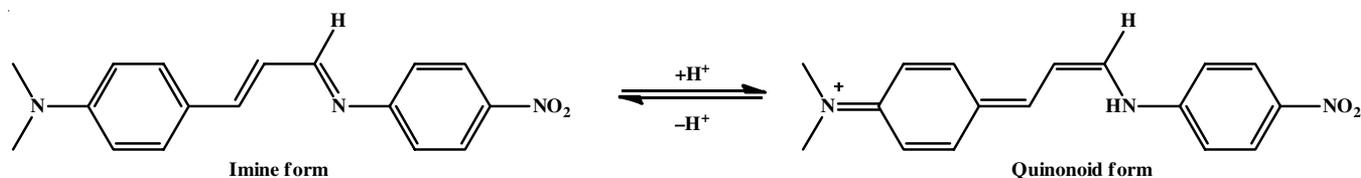
Scheme-II: Tautomeric conversion of **P1** in an acidic medium

tion found from the DFT calculations. Further, the conversion of imine to quinonoids form is manifested from the distinct isosbestic point at $\lambda \approx 482$ nm, which indicates the presence of an equilibrium existing in the absorption spectrum of **P1** (Fig. 1). The spectral shift from 414 nm to 558 nm (≈ 144 nm) was found for the conversion of imine to quinonoids form of **P1**. Thus, one can argue that the prepared **P1** receptor exhibits better sensing property than the sensor because the colour change can be observed with naked eyes in case of chemosensor **P1**. A close inspection of the UV-vis spectra suggests that the addition of small amount of acetic acid to the receptor solution in acetonitrile results in a small increase in absorbance which leads to the imine form along with a small red shift. This can mainly be attributed to the enhancement of polarity of the less polar solvent (acetonitrile) by the addition of acid (acetic acid).

As a result, the receptor **P1** shows a better colour in the solution. A large amount of acid source *viz.* trifluroacetic acid or acetic acid is required for the complete titration *i.e.* the conversion of imine to quinonoids form in less polar solvents as compared to the aqueous solvents. This is attributed to the facilitated ionization of acids in polar solvents, leading to a higher degree of dissociation compared to less polar solvents. Moreover, compared to other indicators, the prepared indicator **P1** exhibits good acid sensitivity in non-polar solvents.

The synthesized **P1** indicator exhibits excellent solubility in less polar solvents, specifically acetonitrile (ACN) and demonstrates high sensitivity to acids in these solvents. This characteristic makes it a promising candidate for the colorimetric detection of a trace amount of the acids in non-aqueous solvents. The results obtained from these real-time paper strip

TABLE-1
λ_{max} (nm) VALUES WITH CORRESPONDING EXCITATION ENERGY (eV), OSCILLATOR FREQUENCY, TRANSITION
INVOLVED (MAJOR) AND EXTENT OF CONTRIBUTION OBTAINED AT B3LYP-GD3/6-31++G(d,p) LEVEL OF THEORY

System	Wavelength (nm)	eV	f	Transition	Contribution
P1	419.9 (s)	2.95	0.96	HOMO → LUMO+1	0.65
	580.0 (w)	2.14	0.67	HOMO → LUMO	0.71
P1H-O	490.7 (w)	2.52	0.70	HOMO-1 → LUMO	0.49
	682.0 (s)	1.82	1.44	HOMO → LUMO	0.71
P1H	515.3	2.41	1.61	HOMO → LUMO	0.70
P1H-N	299.7 (w)	4.14	0.23	HOMO-1 → LUMO+1	0.63
	411.0 (s)	3.01	1.13	HOMO → LUMO	0.69

test kits further support the high sensitivity and reliability of **P1** as an acid-sensitive indicator. This study presents a significant theoretical advancement in the synthesis of multiple acid indicators in non-aqueous solvents. The combination of experimental evidences and theoretical aspects underscore the importance and promising applications of the findings in the field of acid-base chemistry and analytical techniques for the non-aqueous systems.

UV-visible studies: The UV-visible spectra for all the protonated species, with wavelength for the strongest absorption maxima, in acetonitrile is shown in Fig. 2a. Besides, their absorption maxima with the corresponding excitation energies, oscillator frequencies, and major transitions involved and extent of contributions are shown in Table-1. The occurrence of the two absorption maxima for **P1** at 419.9 (s) and 580.0 (w) validates the suitability of chosen theoretical level for the present study. The obtained λ_{max} value corresponds to the excitation energy of 2.95 eV with the oscillator frequency of 0.96 and this can be attributed to 65% (major) contribution from the HOMO→LUMO+1 transition. After protonation, the strongest absorption maxima for **P1H-O**, **P1H** and **P1H-N** are obtained at 682.0, 515.3 and 411.0 nm, respectively. However, the experimental λ_{max} value for the protonated species is obtained at 558 nm, which is considerably close to the theoretical results calculated for **P1H**. Thus, it can conclusively be suggested that the protonation occurs primarily at N-atom of enamine. On the other hand, the absorption maximum corresponds to the excitation energy of 2.41 eV and oscillator frequency of 1.61 can be attributed to 70% (major) contribution from the HOMO→LUMO

transition. The Frontier Molecular Orbital (FMO) for **P1** and **P1H** with the major modes of transition are shown in Fig. 2b-c.

NMR studies: NMR spectrum of a systems is quite useful in predicting the chemical environment around its particular atom and therefore, NMR spectra of the deprotonated and all possible protonated species are estimated theoretically at B3LYP/6-311++G(2d,p)level of theory. For ^1H, ^{15}N and ^{17}O NMR studies TMS, NH_3 and H_2O were utilized as the references respectively and the estimated chemical shift values (δ in ppm) are shown in Table-2. In the deprotonated species, the δ-values for protonation at the probable sites *viz.* O-atom of NO_2 group, N-atom of enamine group, N-atom attached with two Me-groups were found to be 630.8, 342.9 and 80.7 ppm, respectively. Upon protonation, the protonated sites are seemed to undergo considerable shift towards 330.7 (**P1H-O**), 161.5 (**P1H**) and 87.7 (**P1H-N**) ppm. Moreover, the δ-values for the proton present at **P1H-O**, **P1H** and **P1H-N** were found to be 8.1, 7.9 and 5.5 ppm, respectively. Experimental proton NMR study performed

TABLE-2
CHEMICAL SHIFT (δ) VALUES (IN ppm) FOR ^1H, ^{15}N
AND ^{17}O NMR SPECTRA OF THE DEPROTONATED
AND PROTONATED SPECIES OBTAINED AT
B3LYP/6-311++G(2d,p) LEVEL OF THEORY

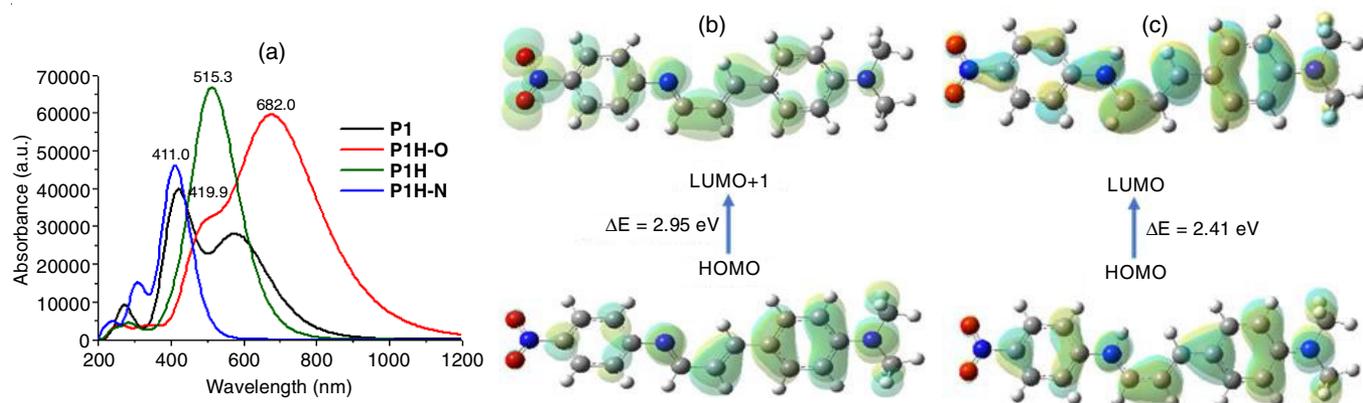| System	^1H (Ref$_{TMS}$)	N-25 (Ref$_{NH3}$)	O-37 (Ref$_{H2O}$)	N-11 (Ref$_{NH3}$)
P1	–	342.9	630.8	80.7
P1H-O	8.41	344.96	330.7	123.7
P1H	7.92	161.5	653.1	129.8
P1H-N	5.47	393.02	647.9	87.7

Fig. 2. UV-vis absorption spectra of (a) **P1**, **P1H-O**, **P1H** and **P1H-N** in acetonitrile, major modes of transition with the frontier molecular orbitals of (b) **P1** and (c) **P1H**

on the protonated species found the δ-value of 261.0 ppm, which is quite close to the result, obtained for **P1H**. Thus, the experimental NMR spectroscopic result appears to be supplementary to its theoretical result and both these studies collectively suggest that the protonation is highly likely at the N-atom of the enamine group. Earlier findings on the similar type of species also support in favour of the result in the present study.

Theoretical validation: To predict the possible sites for protonation the natural bond orbital (NBO) analysis was carried out [18]. Fig. 3 shows the calculated NBO charge for cinnamaldehyde derivative (**P1**). The O-atom of NO_2 group, N-atom of enamine group and N-atom containing two methyl groups bear negative charge of -0.397, -0.473 and -0.456 e^-, respectively. It has been an established fact that the tendency of protonation usually increases with increase in the negative charge. Although, all these three sites, each bearing sufficient negative charge, to be protonated, the N-atom of enamine group with the maximum negative charge is probably the most favourable site for protonation.
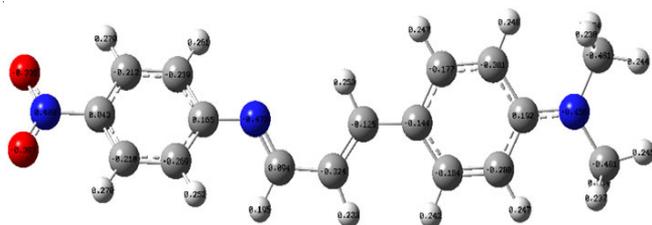

Fig. 3. NBO charge for **P1** calculated at B3LYP-GD3/6-31++G(d,p) level of theory

Electronic energy, interaction energy, enthalpy and free energy changes: The geometries of all the protonated species *viz.* the species protonated at O-atom of NO_2 group (**P1H-O**), at N-atom of enamine (**P1H**) and N-atom with two Me-groups (**P1H-N**) are optimized which along with their corresponding electronic energies are shown in Fig. 4. The real minima are obtained for all the protonated species with the lowest harmonic vibrational frequencies of 23.65 (**P1H-O**), 24.37 (**P1H**) and 26.60 (**P1H-N**) cm^{-1}, respectively. Besides, all the protonated species are arguably found to be more stable with higher negative electronic energies compared to their deprotonated counterparts (Table-3). This suggests the possible protonation at all the sites bearing negative charge. Amongst the protonated species, **P1H** is the most stable one because it possesses more negative electronic energy (-610641.09 kcal mol^{-1}) than the other two. This is in agreement with the NBO charge calculation which has revealed that **P1**, the deprotonated species of **P1H**, with higher charge has a greater tendency to get protonated.
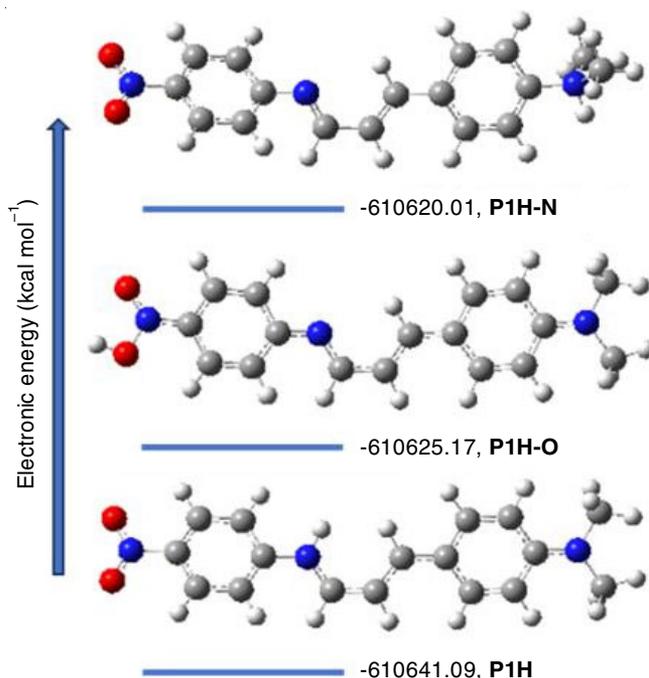

Fig. 4. Electronic energies for the protonated species obtained at B3LYP-GD3/6-31++G(d,p) level of theory

The interaction energy (IE) is known to manifest the strength of an interaction, while the change in the enthalpy (ΔH) and free energy (ΔG) reflect the thermodynamic driving force and feasibility of an interaction. Therefore, these quantities are estimated for the process of protonation and the results are presented in Table-3. Based on the electronic energy estimation, the species **P1H** has the greatest negative ionization energy value of -77.64 kcal mol^{-1}, suggesting the strongest interaction. The calculated values for both the thermodynamic quantities, *viz.* ΔH and ΔG are negative which reflect that the protonation is a spontaneously occurring exothermic process. Moreover, the ΔH and ΔG values for the spices **P1H** are found to be -58.19 and -56.94 kcal mol^{-1}, respectively which are more negatives than that of the other two species **P1H-O** and **P1H-N**. Thus, it is unambiguous that the protonation is most favourable at the N-atom of enamine group.

Reversibility and sensor performance of receptor P1: In this study, the reversibility of receptor **P1** was thoroughly evaluated, subjecting it to an alternate addition of acid and basic. Present analysis involves monitoring the changes in absorbance at some specific wavelengths using UV-visible spectroscopic technique (Fig. 5). Upon addition of acid, an increase in absorbance at 372 nm and a decrease at 558 nm was observed accompanied by a colour shift from yellowish to pinkish in the solution. To validate the reversibility, the same concentrated trimethylamine (TEA) solution was reintroduced to **P1** + acid containing solution. Remarkably, the spectra almost reverted back to their original state and the solution colour changed from pinkish to yellowish again (Fig. 5). Additionally, the absorbance intensity was restored once more in the additional studies that involved adding acid to the solution, demonstrating that receptor **P1** for the acids is reversible. This observation provides strong evidence that the proposed system can

TABLE-3
CHANGE IN INTERACTION ENERGY (IE),
ENTHALPY (ΔH) AND FREE ENERGY (ΔG)

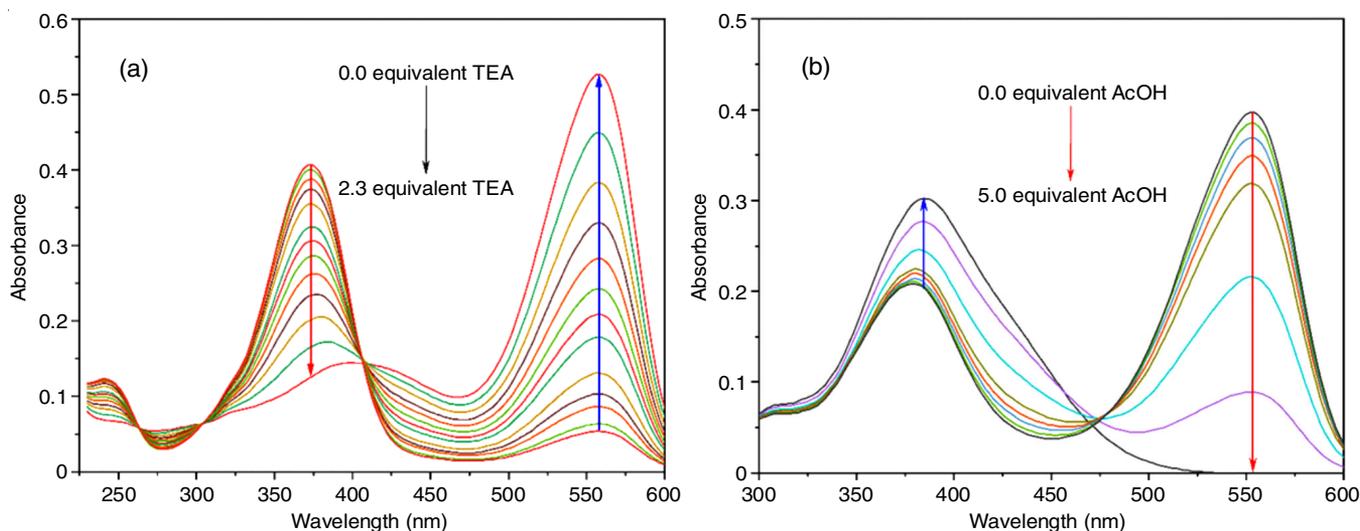| System	IE (kcal mol^{-1})	ΔH (kcal mol^{-1})	ΔG (kcal mol^{-1})	$^1H/^{14}N$ NMR
P1H-O	-61.71	-43.31	-41.91	–
P1H	-77.64	-58.19	-56.94	–
P1H-N	-56.56	-35.87	-34.57	5.5/87.7

Fig. 5. Reversible UV-vis spectra of (**P1** + TFA) complex and (**P1** + AcOH) complex with TEA, respectively

serve as a promising reversible colorimetric sensor. Overall, these findings demonstrated the potential utility of the developed receptor **P1** in reversible colorimetric sensing applications, highlighting its significance in various sensor-based technologies.

Test strips for the detection of trifluoroacetic acid: In this study, the practical application of compound **P1** was investigated using Whatman-41 filter paper strips as the experimental platform. The strips were soaked in a concentrated solution of **P1** in acetonitrile and subsequently dried at room temperature. Initially, the strips exhibited a yellow colour. However, upon exposure to trifluoroacetic acid (TFA) solutions with varying concentrations, a distinctive colour change from yellow to pink was observed (Fig. 6). This colour change was specifically observed for trifluoroacetic acid concentrations within the range up to 10 ppm. The transformation of colour is attributed to the formation of a quinonoid form, which corresponds to the **P1** + H$^+$ complex.
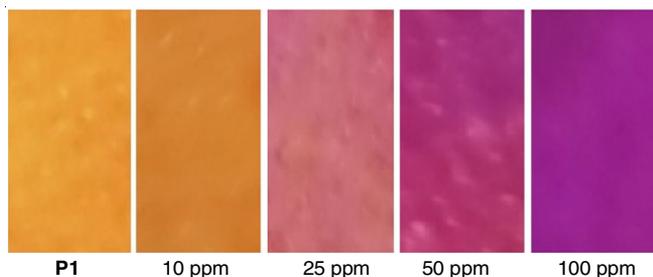

Fig. 6. Schematic representation of the preparation of test strips and colour changes of **P1** upon the addition of different concentrations of TFA

Conclusion

A 4-aminophthalimide-adorned acid sensor (**P1**) incorporating an electron donor-acceptor subunit was sucessfully developed. The theoretical aspect of the proposed sensor involves their potential ability to detect acids in non-aqueous solvents. Experimentally, the as-prepared **P1** sensor display remarkable sensitivity to acids, manifesting a distinct colour change that is easily observable to the naked eye. This colour

change is evident as the sensor transition from yellow to pink upon exposure to acids. Additionally, a colorimetric paper strip based on this acid sensor was also developed. This paper strip demonstrates the capability to detect trace amounts of acids in non-aqueous solvents, broadening the application of the proposed sensor beyond acid detection alone. Furthermore, the developed sensor has proven effective in determining water concentration in aqueous media, highlighting their versatility as analytical tools.

CONFLICT OF INTEREST

The authors declare that there is no conflict of interests regarding the publication of this article.

REFERENCES

1. M.P. Gashti, J. Asselin, J. Barbeau, D. Boudreau and J.A. Greener, *Lab Chip*, **16**, 1412 (2016);
https://doi.org/10.1039/C5LC01540E
2. S. Liu, Z. Zhang, Q. Liu, H. Luo and W. Zheng, *J. Pharm. Biomed. Anal.*, **30**, 685 (2002);
https://doi.org/10.1016/S0731-7085(02)00356-4
3. K.-H. Kim, W.-C. Shin, Y.-S. Park and S.-S. Yoon, *Food Sci. Biotechnol.*, **16**, 99 (2007).
4. M.J. Kim, S.W. Jung, H.R. Park and S.J. Lee, *J. Food Eng.*, **113**, 471 (2012);
https://doi.org/10.1016/j.jfoodeng.2012.06.018
5. A. Brandenburg, R. Edelhauser, T. Werner, H. He and O.S. Wolfbeis, *Mikrochim. Acta*, **121**, 95 (1995);
https://doi.org/10.1007/BF01248244
6. A. Markovics, G. Nagy and B. Kovacs, *Sens. Actuators B Chem.*, **139**, 252 (2009);
https://doi.org/10.1016/j.snb.2009.02.075
7. P.T. Snee, R.C. Somers, G. Nair, J.P. Zimmer, M.G. Bawendi and D.G. Nocera, *J. Am. Chem. Soc.*, **128**, 13320 (2006);
https://doi.org/10.1021/ja0618999

8. G. Wirnsberger, B.J. Scott and G.D. Stucky, *Chem. Commun.*, **119**, 119 (2001);
    https://doi.org/10.1039/b003995k

9. K. Abe, K. Suzuki and D. Citterio, *Anal. Chem.*, **80**, 6928 (2008);
    https://doi.org/10.1021/ac800604v

10. S.T. Lee, J. Gin, V.P.N. Nampoori, C.P.G. Vallabhan, N.V. Unnikrishnan and P. Radhakrishnan, *J. Opt. A, Pure Appl. Opt.*, **3**, 355 (2001);
    https://doi.org/10.1088/1464-4258/3/5/307

11. F.R. Zaggout, *J. Dispers. Sci. Technol.*, **26**, 757 (2005);
    https://doi.org/10.1081/DIS-200063087

12. S. Jurmanovic, S. Kordic, M.D. Steinberg and I.M. Steinberg, *Thin Solid Films*, **518**, 2234 (2010);
    https://doi.org/10.1016/j.tsf.2009.07.158

13. R. Makote and M.M. Collinson, *Anal. Chim. Acta*, **394**, 195 (1999);
    https://doi.org/10.1016/S0003-2670(99)00305-0

14. P. Kassal, R. Surina, D. Vrsaljko and I.M. Steinberg, *J. Sol-Gel Sci. Technol.*, **69**, 586 (2014);
    https://doi.org/10.1007/s10971-013-3261-9

15. Y. Hiruta, N. Yoshizawa, D. Citterio and K. Suzuki, *Anal. Chem.*, **84**, 10650 (2012);
    https://doi.org/10.1021/ac302178z

16. O.S. Wolfbeis, *Anal. Chem.*, **78**, 3859 (2006);
    https://doi.org/10.1021/ac060490z

17. M.I.J. Stich, L.H. Fischer and O.S. Wolfbeis, *Chem. Soc. Rev.*, **39**, 3102 (2010);
    https://doi.org/10.1039/b909635n

18. P.C.A. Jeronimo, A.N. Araujo and M.C.B.S.M. Montenegro, *Talanta*, **72**, 13 (2007);
    https://doi.org/10.1016/j.talanta.2006.09.029

19. A.L. Berhanu, Gaurav, I. Mohiuddin, A.K. Malik, J.S. Aulakh, V. Kumar and K.-H. Kim, *Trends Analyt. Chem.*, **116**, 74 (2019);
    https://doi.org/10.1016/j.trac.2019.04.025

20. M.-M. Wang, Y.-J. Zheng, T. Jing, J.-Z. Tian, P.-S. Chen, M.-Y. Dong, C. Wang, C. Yan, C. Liu, T. Ding, W. Xie and Z.-H. Guo, *Sci. Adv. Mater.*, **11**, 756 (2019);
    https://doi.org/10.1166/sam.2019.3526

21. K. Behera, S. Pandey, A. Kadyan and S. Pandey, *Sensors*, **15**, 30487 (2015);
    https://doi.org/10.3390/s151229813

22. M.C. Buzzeo, C. Hardacre and R.G. Compton, *Anal. Chem.*, **76**, 4583 (2004);
    https://doi.org/10.1021/ac040042w

23. Z. Rahman, M. Rajbanshi, M. Mahato, S. Ghanta and S.K. Das, *J. Mol. Liq.*, **359**, 119365 (2022);
    https://doi.org/10.1016/j.molliq.2022.119365

24. W.S. Matthews, J.E. Bares, J.E. Bartmess, F.G. Bordwell, F.J. Cornforth, G.E. Drucker, Z. Margolin, R.J. Mccallum, G.J. Mccollum and N.R. Vanier, *J. Am. Chem. Soc.*, **97**, 7006 (1975);
    https://doi.org/10.1021/ja00857a010

25. A. Kutt, S. Selberg, I. Kaljurand, S. Tshepelevitsh, A. Heering, A. Darnell, K. Kaupmees, M. Piirsalu and I. Leito, *Tetrahedron Lett.*, **59**, 3738 (2018);
    https://doi.org/10.1016/j.tetlet.2018.08.054

26. E. Rossini, A.D. Bochevarov and E.W. Knapp, *ACS Omega*, **3**, 1653 (2018);
    https://doi.org/10.1021/acsomega.7b01895

27. S.N. Park, H. Kim, K. Kim, J.A. Lee and D.-S. Lho, *Phys. Chem. Chem. Phys.*, **1**, 1893 (1999);
    https://doi.org/10.1039/a900248k

28. T. Matsui, T. Baba, K. Kamiya and Y. Shigeta, *Phys. Chem. Chem. Phys.*, **14**, 4181 (2012);
    https://doi.org/10.1039/c2cp23069k

29. A. Kutt, I. Leito, I. Kaljurand, L. Soovali, V.M. Vlasov, L.M. Yagupolskii and I.A. Koppel, *J. Org. Chem.*, **71**, 2829 (2006);
    https://doi.org/10.1021/jo060031y

30. I.M. Kolthoff, S. Bruckenstein and M.K. Chantooni Jr., *J. Am. Chem. Soc.*, **83**, 3927 (1961);
    https://doi.org/10.1021/ja01480a001

31. G. Garrido, E. Koort, C. Rafols, E. Bosch, T. Rodima, I. Leito and M. Roses, *J. Org. Chem.*, **71**, 9062 (2006);
    https://doi.org/10.1021/jo061432g

32. H.-S. Kim, T.D. Chung and H. Kim, *J. Electroanal. Chem.*, **498**, 209 (2001);
    https://doi.org/10.1016/S0022-0728(00)00413-7

33. W.C. Barrette, H.W. Johnson and D.T. Sawyer, *Anal. Chem.*, **56**, 1890 (1984);
    https://doi.org/10.1021/ac00275a030

34. C. Reichardt, *Chem. Rev.*, **94**, 2319 (1994);
    https://doi.org/10.1021/cr00032a005

35. G. Jakab, C. Tancon, Z. Zhang, K.M. Lippert and P.R. Schreiner, *Org. Lett.*, **14**, 1724 (2012);
    https://doi.org/10.1021/ol300307c

36. I.M. Kolthoff, M.K. Chantooni and S. Bhowmik, *Anal. Chem.*, **39**, 315 (1967);
    https://doi.org/10.1021/ac60247a047

37. S. Wakabayashi, Y. Kato, K. Mochizuki, R. Suzuki, M. Matsumoto, Y. Sugihara and M. Shimizu, *J. Org. Chem.*, **72**, 744 (2007);
    https://doi.org/10.1021/jo061684h

38. M.J. Frisch, G.W. Trucks, H.B. Schlegel, G.E. Scuseria, M.A. Robb, J.R. Cheeseman, G. Scalmani, V. Barone, G.A. Petersson, H. Nakatsuji, X. Li, M. Caricato, A.V. Marenich, J. Bloino, B.G. Janesko, R. Gomperts, B. Mennucci, H.P. Hratchian, J.V. Ortiz, A.F. Izmaylov, J.L. Sonnenberg, D. Williams-Young, F. Ding, F. Lipparini, F. Egidi, J. Goings, B. Peng, A. Petrone, T. Henderson, D. Ranasinghe, V.G. Zakrzewski, J. Gao, N. Rega, G. Zheng, W. Liang, M. Hada, M. Ehara, K. Toyota, R. Fukuda, J. Hasegawa, M. Ishida, T. Nakajima, Y. Honda, O. Kitao, H. Nakai, T. Vreven, K. Throssell, J.A. Montgomery Jr., J.E. Peralta, F. Ogliaro, M.J. Bearpark, J.J. Heyd, E.N. Brothers, K.N. Kudin, V.N. Staroverov, T.A. Keith, R. Kobayashi, J. Normand, K. Raghavachari, A.P. Rendell, J.C. Burant, S.S. Iyengar, J. Tomasi, M. Cossi, J.M. Millam, M. Klene, C. Adamo, R. Cammi, J.W. Ochterski, R.L. Martin, K. Morokuma, O. Farkas, J.B. Foresman and D.J. Fox, Gaussian, Inc., Gaussian 16, Revision A.03, Wallingford CT (2016).

39. B. Saha and P.K. Bhattacharyya, *Phy. Sci. Rev.*, **8**, 793 (2023);
    https://doi.org/10.1515/psr-2020-0086

40. S. Grimme, A. Hansen, J.G. Brandenburg and C. Bannwarth, *Chem. Rev.*, **116**, 5105 (2016);
    https://doi.org/10.1021/acs.chemrev.5b00533

41. B. Saha and P.K. Bhattacharyya, *New J. Chem.*, **47**, 12790 (2023);
    https://doi.org/10.1039/D3NJ01797D

42. J. Tomasi, B. Mennucci and R. Cammi, *Chem. Rev.*, **105**, 2999 (2005);
    https://doi.org/10.1021/cr9904009

43. T. Helgaker, S. Coriani, P. Jorgensen, K. Kristensen, J. Olsen and K. Ruud, *Chem. Rev.*, **112**, 543 (2012);
    https://doi.org/10.1021/cr2002239

44. A.E. Reed, L.A. Curtiss and F. Weinhold, *Chem. Rev.*, **88**, 899 (1988);
    https://doi.org/10.1021/cr00088a005